1/F NOISE CONSIDERATIONS FOR THE DESIGN AND PROCESS OPTIMIZATION OF PIEZORESISTIVE CANTILEVERS

J. A. Harley and T. W. Kenny
Dept. of Mechanical Engineering, Stanford University

ABSTRACT

Piezoresistive cantilevers are limited by two major noise sources: Johnson noise, which is independent of frequency, and conductance fluctuation noise, which has a *1/f* spectrum. The *1/f* fluctuations of piezoresistive cantilevers are shown to vary inversely with the total number of carriers in the piezoresistor, as formulated by F.N. Hooge [Phys. Rev. Lett., 1969]. While *1/f* noise is therefore reduced for large, heavily doped cantilevers, sensitivity considerations favor thin, lightly doped cantilevers. Balancing these conflicting constraints produces optima for many design and processing parameters. For a cantilever with specified spring constant and bandwidth requirements, optima are identified for the beam thickness and length, and it is shown that the legs should be between 1/3 and 2/3 of the total length with a doping depth that is 1/3 of the beam thickness. Additionally, an optimal doping concentration is identified as a function of the cantilever volume and the measurement bandwidth. Annealing reduces *1/f* noise but causes a loss in sensitivity due to dopant diffusion, and an optimal anneal is computed with a typical diffusion length 10^{-6} cm. The analysis, methods and some of the conclusions from this work are also applicable to other types of piezoresistive sensors.

INTRODUCTION

Piezoresistive detection is a popular technique when simple integrated sensors are required, and is often used for atomic force microscope (AFM) cantilevers instead of conventional optical detection. The convenience of a piezoresistive cantilever comes at the expense of resolution, however, so they are primarily used in cases where laser detection is difficult. These include high-vacuum AFM[1], large arrays of cantilevers[2], ultra-small high-bandwidth cantilevers[3], and portable cantilever-based sensors[4,5]. Our objective with this work is to enable the construction of piezoresistive cantilevers that are competitive with the resolution of optically detected devices.

All piezoresistive sensors have the same fundamental trade-offs between sensitivity and noise, and for optimum resolution the effects of design and process decisions on both of these factors must be understood. The issues regarding piezoresistor sensitivity were well analyzed by Tortonese in his 1993 thesis[6], but although there have been papers on piezoresistor noise[7,8], the practical design implications have not been fully examined.

Piezoresistive sensors have two main noise sources, both easily distinguishable on a typical noise spectrum vs. frequency, as shown in Figure 1. At low frequencies, all resistors suffer from conductance fluctuations, usually called *1/f* noise because the noise power density [V^2/Hz] increases as one over the frequency. Added to this is Johnson noise, which is independent of frequency. Johnson noise is fundamental, due to thermal energy in a resistor, and is well understood[9].

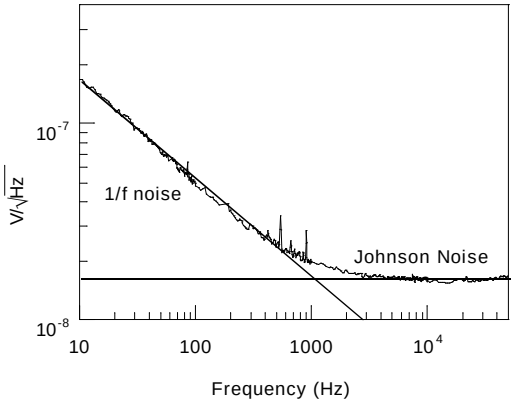

Figure 1. Typical cantilever noise spectrum showing Johnson and *1/f* noise.

The cause of *1/f* noise, on the other hand, is still an active area of research, so despite the fact that it is dominant for most piezoresistors, it has not previously been included in an optimization. Recently, however, a 30 year-old empirical model of *1/f* noise in a resistor[10] was shown to be applicable for piezoresistors[11]. This model has clear dependencies on the sensor geometry and processing, and introduces design and processing trade-offs which lead to well-defined optima for many of the design issues.

The optimization analysis in this paper will be focused on diving-board piezoresistive cantilevers because of their simple geometry and quantifiable performance metrics. The methods and most of the results from this analysis should, however, be directly applicable to other types of piezoresistive sensors, including commercially available pressure sensors and accelerometers.

PERFORMANCE PARAMETERS

For a cantilever, the important performance parameters are sensitivity (either for displacement or force), noise, bandwidth and spring constant. The

resolution is given by the noise over the sensitivity. These parameters are dealt with separately below.

All subsequent calculations will assume a cantilever with the design shown in Figure 2. The cantilever has two legs of length l_{leg} which extend some fraction of the total length l. The total thickness of the cantilever is t, with a top layer of thickness t_d doped to a concentration p. The width of the cantilever legs is $w/2$, and the split between the two legs is assumed to be of negligible width, so that the total cantilever width is ~w.

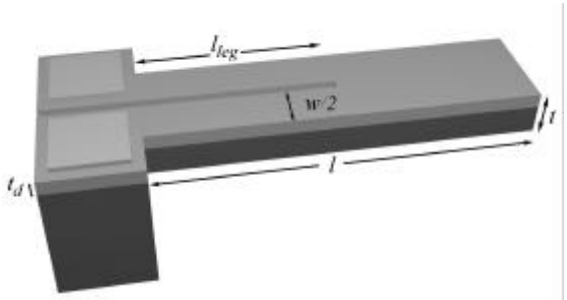

Figure 2. Schematic of cantilever dimensions. The cantilever has length l, leg length l_{leg}, width w, thickness t and a p-type piezoresistive top layer of thickness t_d.

Although this cantilever design is not identical to an actual device pictured in Figure 3, the differences are inconsequential for the optimization. A force F applied at the end of a cantilever introduces a moment a distance y from the base that is only dependent on the area moment of inertia I_A at y, according to

$$s = \frac{F(l-y)c}{I_A}. \qquad (1)$$

Since the leg width was used to define w, $I_A = wt^3/12$ for the two legs, and the minimum detectable force for the cantilevers of Figure 3 and Figure 2 will be the same. Differences in the spring constant k between the ideal and actual beam can be included when deriving the minimum detectable displacement from the minimum detectable force. For this reason the derivations are provided in terms of force sensitivity and resolution, and the spring constant (which can be corrected for deviations from the model cantilever) is used to convert to displacement sensitivity or resolution. There may be also differences in the resonant frequency between the real and ideal cantilever, but they do not affect the conclusions of this analysis.

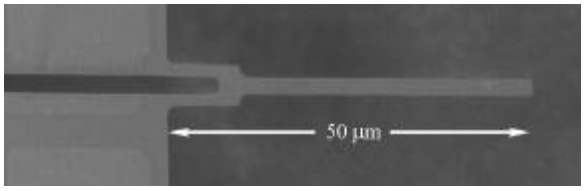

Figure 3. SEM micrograph of 950 Å-thick piezoresistive cantilever. The spring constant is 0.001 N/m with a resonant frequency of 50 kHz.

A table of the variables used in this paper can be found in Table 1.

Sensitivity

Stress in a semiconductor changes the resistivity[12]. An applied stress, s, along the longitudinal axis of the crystal causes a change in resistivity according to the equation

$$\frac{\Delta r}{r} = p_l s \qquad (2)$$

where r is the resistivity and p_l is the longitudinal piezoresistive coefficient. Following the derivation by Tortonese[6], if the stress distribution is known, the fractional resistance change of a flexed cantilever beam can be computed by integrating to find the conductivity as a function of the load. The maximum stress occurs at the beam surface, or $c=t/2$, giving a fractional resistance change of

$$\frac{\Delta R}{R} = \frac{6p_l\left(l - l_{leg}/2\right)}{wt^2}F. \qquad (3)$$

By including the spring constant, which for a simple cantilever is

$$k = \frac{Ewt^3}{4l^3}, \qquad (4)$$

the sensitivity to a displacement is found to be

$$\frac{\Delta R}{R} = \frac{3p_l Et\left(l - l_{leg}/2\right)}{2l^3}x. \qquad (5)$$

Since the spring constant equation is linear in w, equation (5)also holds true for the beam of Figure 2 divided into two legs by a slit of negligible width.

Equation (3) is simplified by the assumption that the stress is measured at the surface where it is maximized. In a real cantilever, the dopant is distributed throughout the beam, and the doped region near the neutral axis does not experience any stress. Since the dopant at the neutral axis contributes to the conductivity but not to the signal, equation (3) states the maximum possible sensitivity for an infinitely thin doped layer at the surface.

For a better model of the total fractional resistance change, Tortonese formulated an efficiency factor b to be inserted in the numerator of the sensitivity equation[6]. b is computed as the ratio of the complete $\Delta R/R$, which includes the distribution of the stress

and dopant, to the simplified version in equations (3) and (5) in which the stress is assumed to be at the surface value. It is defined as follows:

$$b = \frac{2}{t}\frac{\int_{-t/2}^{t/2} p_l(p)m_p(p)\,p\,c\,dc}{\int_{-t/2}^{t/2} p_l(p)m_p(p)\,p\,dc}. \qquad (6)$$

Both the piezoresistive coefficient, p_l, and the hole mobility, m_p, are functions of the dopant concentration p. A p-type dopant is assumed, since it provides high sensitivity in the [110] direction, a convenient crystallographic orientation from a fabrication standpoint.

Noise

Johnson Noise

The Johnson noise of a piezoresistor is a fundamental performance limit, set by the thermal energy of the carriers in a resistor, and dependent only on the resistance, R, and the temperature, T. It is 'white noise', with a spectral density that is independent of frequency. The voltage noise power density (units [V^2/Hz]) is

$$S_J = 4k_BTR. \qquad (7)$$

For a step dopant profile, the total Johnson noise depends only on the geometry and the doping, since for the geometry given in Figure 2 the resistance is approximated by $R=(4l_{leg}r)/(wt_d)$. The resistivity of the doped region is defined as $r=(m_pqp)^{-1}$, where m_p is a known function of the dopant density. The factor of 4 enters because the cantilever has two legs, each of width $w/2$ and length l_{leg}. Then the total Johnson noise power for a given geometry and doping in a bandwidth from f_{min} to f_{max} is

$$\overline{V_J^2} = \frac{16k_BTl_{leg}}{wt_dm_pqp}(f_{\max} - f_{\min}). \qquad (8)$$

Hooge Noise

In 1969, F. N. Hooge put forth the empirical observation that the *1/f* voltage noise power spectral density (units [V^2/Hz]) of a homogeneous resistor is dependent on the total number of carriers in the resistor, according to the equation

$$S_H = \frac{aV_B^2}{Nf}, \qquad (9)$$

where V_B is the bias voltage across a resistor with a total number of carriers N, and f is frequency[10]. The variable a is a dimensionless parameter which, for an implanted resistor, has been found to vary depending on the anneal[13]. Although there may be other sources of *1/f* noise, equation (9) imposes a lower bound that is important for cases where this noise source is large (N is small) or where all other *1/f* sources have been reduced. Data will be shown which indicates that for piezoresistors Hooge noise is usually the limiting *1/f* noise source.

If equation (9) is integrated from f_{min} to $f_{max,}$ then the voltage noise power is

$$\overline{V_H^2} = \frac{aV_B^2}{N}\ln\left(\frac{f_{\max}}{f_{\min}}\right). \qquad (10)$$

For a rectangular resistor with constant doping concentration, the number of carriers is the doping density times the resistor volume, so the *1/f* noise power density varies inversely with the volume and the doping concentration. The noise is not dependent on the resistance, however, since a short, wide resistor with low resistance can have the same number of carriers as a long, narrow resistor with high resistance. Note that for any decade of frequency, the integrated *1/f* noise is constant.

For resistors where the current density is not constant, such as the cantilever of Figure 3, the simple formula of equation (9) cannot be directly applied. Although the beam is doped along its full length, carriers near the tip of the cantilever are not involved in the conduction and do not contribute to reduced Hooge noise. The appropriate equation, which weights carriers by their contribution to the current density, is[14]:

$$S_{VH} = \frac{ar^2}{pI^2f}\iiint (J\cdot J)^2\,dxdydz. \qquad (11)$$

where p is still the carrier density, I is the total current and J is the current density, generally found using finite element models. The integral is taken over the full volume of the cantilever.

For back-of-the-envelope calculations, the number of carriers may be approximated as the doping density times the doped volume of the legs only ($N=l_{leg}t_dw$). With this approximation, the Hooge noise can be predicted based on only the doping and geometry as

$$\overline{V_H^2} = \frac{a\,V_B^2}{l_{leg}t_dwp}\ln\left(\frac{f_{\max}}{f_{\min}}\right). \qquad (12)$$

We have recently verified the Hooge noise relation for piezoresistors by calculating the total number of carriers from a finite element model and equation (11), and measuring the *1/f* noise for a variety of cantilevers. This data is shown in Figure 4. The plot shows noise data from cantilevers of different lengths, widths and thicknesses, ranging from 900 Å to 2.2 μm thick. The square points are for 0.1 μm-thick cantilevers we have fabricated with 300 Å-thick $4\cdot10^{19}$ cm^{-3} boron doped epitaxially grown layers. The lengths range from 10 μm to 350 μm and the widths from 4 μm to 40 μm.

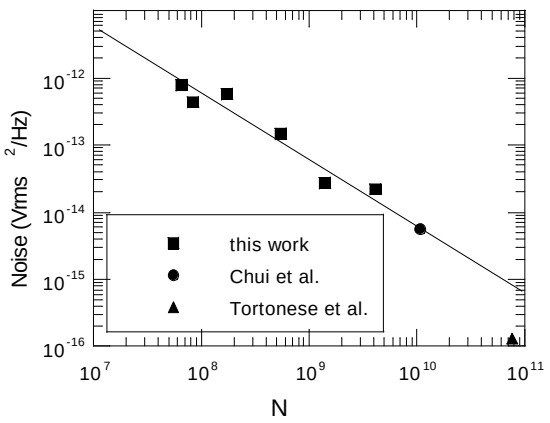

Figure 4. Measured 1/f noise power density at 10 Hz vs. number of carriers for piezoresistive cantilevers. A line of slope -1 indicates the Hooge model. The point from Tortonese et al. has a greater anneal than the others.

This plot contradicts the notion that surface quality is paramount in the *1/f* noise level of a resistor, since the data shows increasing noise as the surface area decreases. If the hypothesis were put forth that the surface to volume *ratio* were the important parameter, then cantilevers with constant thickness and doping should all have the same noise, because their surface to volume ratio, *(wl)/(wlt),* is constant. The square points plotted in Figure 4 are from cantilevers of the same thickness and doping, indicating this is also not the case. For these cantilevers with constant doping density, the *1/f* noise scales as one over the volume, as predicted by the Hooge model.

Thermomechanical Noise

Another possible noise source for consideration in piezoresistive cantilevers is thermomechanical noise. This is the mechanical analog of Johnson noise, and consists of physical oscillations due to thermal energy in the beam. The voltage noise power spectral density is independent of frequency, and has amplitude[15]

$$S_{th} = \frac{4kk_BTB}{w_0 Q} \tag{13}$$

where k is the cantilever stiffness, k_B is Boltzmann's constant, w_0 is the resonant frequency in radians, T is the temperature and S_{th} has units of Newtons squared per Hertz.

The motion resulting from this force noise is greatest at the cantilever resonance, and signals due to thermomechanical noise have been observed above the Johnson noise at resonance in air for piezoresistive cantilevers with sufficiently high Q[3]. In vacuum a resonant peak due to thermomechanical noise is easily detectable for almost any piezoresistive cantilever. Except at resonance, however, this noise source has always been smaller than *1/f* or Johnson noise in practice. Since the measurement bandwidth is typically restricted to frequencies below the first resonance, we will neglect this source of noise in the remainder of the paper.

Bandwidth

The maximum measurement bandwidth is usually set by the resonant frequency of the cantilever, but it is often further reduced with electronic filtering to eliminate excess noise. Since the noise spectrum is integrated over the measurement bandwidth, the frequency range of the measurement determines the total noise.

The choice of the bandwidth may determine which noise source is dominant, and the optimization analysis should be done for a specific frequency range of interest. In non-contact AFM, for example, the signal is only measured in a narrow bandwidth at the cantilever resonant frequency so the *1/f* noise should generally not be an issue and the optimization should focus on the Johnson noise. Similarly, low-frequency measurements will usually be dominated by *1/f* noise.

Spring Constant

The spring constant of the beam, as defined by equation (4), is an important consideration for an AFM cantilever. By choosing a high enough spring constant, a piezoresistive cantilever can be given arbitrarily good position resolution, but the forces required to bend it may be extreme. Similarly, by choosing a soft cantilever, the force resolution can be improved arbitrarily, although this usually comes at the expense of bandwidth.

The disadvantages of an extremely stiff cantilever are readily apparent. For contact AFM imaging, a stiff cantilever exerts large forces which may damage the sample, or result in tip wear. The case of the too-soft spring constant is less obvious, but equally limiting for force measurements. If the force to be measured has a gradient greater than the cantilever spring constant (both have units of N/m), then the cantilever is unstable, and will snap down along the gradient. A similar phenomena causes snap-in for electrostatic actuators commonly used in MEMS devices.

GEOMETRICAL DESIGN OPTIMIZATION

Thickness and length

Cantilever thickness is critical to the performance of the device, and reducing the beam thickness has lead to three substantial performance advances. Thinner cantilevers have increased bending stress from applied forces, and the lower mass permits higher bandwidth for a given spring constant. On two occasions, the thickness of piezoresistive cantilevers was reduced by using thinner implants, a rapid thermal anneal and by avoiding high temperature

steps for the surface passivation[3,16]. A third thickness reduction used epitaxially grown silicon to eliminate transient enhanced diffusion and create a sharper dopant step profile[11].

From the force sensitivity equation (3), it is evident that reducing the thickness will improve the sensitivity, but thickness changes will also affect the spring constant and resonance. Figure 5 illustrates the displacement sensitivity vs. thickness for lines of constant spring constant and resonant frequency, if b is assumed to be one, the legs extend half of the total cantilever length, and the bias voltage is 5 V. To read force sensitivity from this plot, simply divide the displacement sensitivity by the spring constant.

The width of the cantilever in the plot is fixed at 10 μm, and the length is adjusted to achieve the desired spring constant or resonance. Since the contours of fixed spring constant slope upward to the left of the plot, it is evident that improved sensitivity is achieved with thinner, shorter cantilevers.

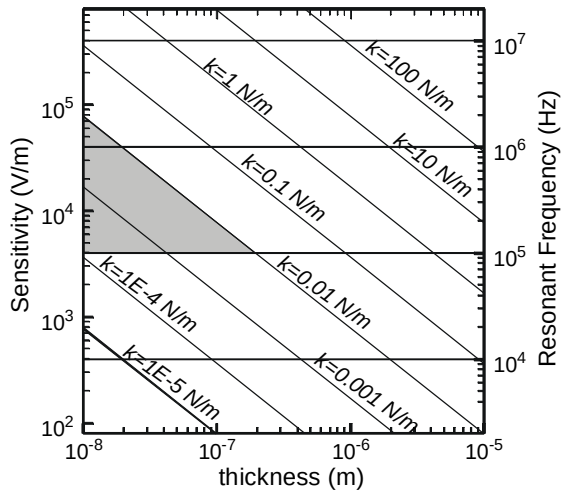

Figure 5. Displacement sensitivity vs. thickness for a 10 μm wide cantilever with given k or f. The horizontal lines are contours of constant resonant frequency. The sloped lines are contours of constant stiffness. The shaded region illustrates the design space for cantilevers with over 100 kHz bandwidth and under 0.01 N/m stiffness.

The sensitivity figure can be used as a design tool when the measurement specifications are given. For example, an AFM cantilever may require a bandwidth of over 100 kHz for high-speed imaging and a spring constant below 0.01 N/m to minimize sample damage. Cantilever dimensions which satisfy these criteria are in the shaded region in Figure 5. At minimum, a cantilever less than 0.2 μm thick is required to meet these requirements.

Leg Length

The overall length of the cantilever is roughly determined once the thickness and spring constant are set. The ratio of the leg length, l_{leg}, to the total length l still remains to be chosen, however. If the legs extend the full length of the cantilever, the number of carriers is maximized, to the benefit of the Hooge noise, but there is a loss in sensitivity due to the extra resistance near the tip of the beam where the stresses are low. Conversely, if the legs had nearly zero length, the piezoresistive region would always see the maximum possible stress, but the resistor would have increased Hooge noise due to a lack of carriers. By writing a full expression for the displacement resolution, the optimum leg length can be computed.

If the piezoresistor makes up one corner of a Wheatstone bridge, the output signal is

$$V_{out} = \frac{V_B}{4}\frac{\Delta R}{R}. \qquad (14)$$

From equations (3), (8), (12), and (14), the minimum detectable force resolution (when the noise equals the sensitivity) can be written as

$$F_{\min} = \frac{\sqrt{\dfrac{aV_B^2}{l_{leg}t_d wp}\ln\left(\dfrac{f_{\max}}{f_{\min}}\right) + \dfrac{16k_B T l_{leg}}{wt_d m_p qp}\left(f_{\max} - f_{\min}\right)}}{\dfrac{3V_B p_l}{2wt^2}\left(\dfrac{l - l_{leg}}{2}\right)}. \qquad (15)$$

In this case the first term in the numerator is the contribution of Hooge noise, and the second is the contribution of Johnson noise.

If l_{leg} in equation (15) is replaced by al, where a is the fraction of the total length that the legs extend, then the resolution can be written as a function of a. Differentiating $F_{\min}$ with respect to a then gives an optimal ratio of the leg extension.

The calculated displacement resolution for a typical cantilever[17] is shown in Figure 6, along with the resolution due to each electrical noise source independently. The *1/f* limited resolution always has a minimum at a=2/3, and the Johnson limited resolution increases monotonically, so there is no reason to extend the legs beyond two thirds of the cantilever length. For leg length less than one third the total length, the *1/f* noise increases dramatically, unless the cantilever is dominated by Johnson noise. For the rest of this work $a=0.5$ will be used as the value for the general case.

Width

Having chosen the length and thickness of the cantilever, there is still some flexibility in the choice of width. From equation (3), it is evident that reducing width can improve force sensitivity and reduce the spring constant, but it has no affect the displacement sensitivity (equation (5)) or resonant frequency. When varying the width while maintaining a fixed cantilever stiffness (i.e. reduce the length at the same time), the net force resolution improves only as $w^{1/6}$, but the resonance increases as $w^{-2/3}$. Resolution gains from a narrow cantilever are

therefore slight, but a narrow cantilever of equivalent spring constant has a significant bandwidth gain. Within the limits of the fabrication technology, narrow cantilevers are preferable.

PROCESSING OPTIMIZATION

At this point, the cantilever geometry has been optimized, but there remain several important processing decisions which will affect the performance. The appropriate doping level must be chosen, as well as the thickness of the doped layer. Following that, surface treatments and an appropriate anneal must be chosen.

There are two major decisions to be made regarding the dopant: 1) how deep should the dopant extend into the cantilever, and 2) what is the appropriate concentration. Both decisions involve a trade-off between sensitivity and noise. The depth optimum is independent of the doping concentration, so it is evaluated first.

Dopant Depth

The optimum depth of the doped layer involves a trade-off of reducing the noise at the expense of the sensitivity. If the doped layer is very shallow, the number of carriers is small and the noise is high, but if the doped layer is very deep, b tends to zero, and sensitivity is lost.

Epitaxially grown layers can achieve step-like doping density profiles, and implanted layers can be approximated as ideal step functions for calculation purposes. Such an assumption simplifies the integral formula of b to $b = 1-t_d/t$. This can be substituted into equation (15) for F_{min}, which can then be differentiated with respect to t_d/t. The minimum resolution occurs for t_d/t=1/3, and is independent of the doping level and the geometry, including thickness. For doping depth between 15% and 60% of the thickness the resolution is within 20% of the optimum, beyond which point it decreases sharply. For all piezoresistive cantilevers, then, the target thickness for the doped layer should be one third of the total thickness, with about a 20% margin for error before the performance is significantly reduced.

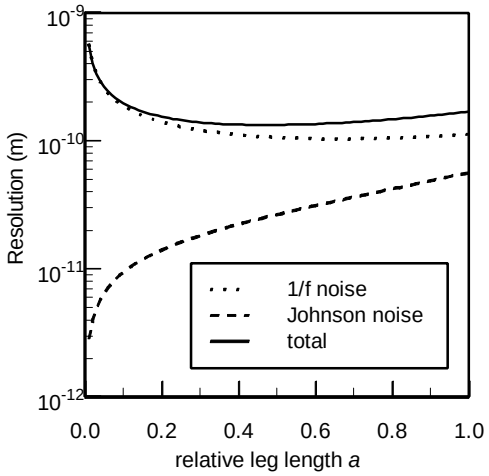

Figure 6. Plot of noise vs. leg length ratio a for standard cantilever[17] in a bandwidth from 10 Hz to 1 kHz.

Dopant Concentration

Early studies of the piezoresistive effect showed that as the doping concentration increased, the piezoresistive coefficient, p_l, decreased[18]. This has a direct impact on the sensitivity from equation(3), and so although a higher concentration has more carriers for reduced noise, it is at the expense of reduced sensitivity.

A majority of recent calculations for the relation between p_l and the doping concentration have used the calculations of Kanda[19]. This model is reasonably accurate at low concentrations, but it substantially underestimates p_l at higher doping concentrations. At low concentrations (~$5\cdot10^{14}$ cm^{-3}) Smith found the p-type longitudinal piezoresistive coefficient in the [110] direction for silicon to be relatively constant at $72\cdot10^{-11}$ m^2/N[12]. Since the piezoresistive coefficient decreases at higher concentrations (above 10^{17} cm^{-3}), a piezoresistive factor $P(p)$ was defined by Kanda which expresses the coefficient as a fraction of this maximum value. Room temperature data from Mason *et al.*[18], from Tufte and Stelzer[20], and one point from Kerr and Milnes[21], is shown in Figure 7 along with the theoretical curve from Kanda.

For concentrations in the range of interest (above 10^{17} cm^{-3}), this data is well approximated by a straight line on the semi-log plot, according to

$$P(p) = \log\left(\frac{b}{p}\right)^a, \qquad (16)$$

with a=0.2014 and b=$1.53\cdot10^{22}$ cm^{-3}.

The trade-off is by now a familiar one. At high dopant concentrations there are many carriers, and therefore improved Hooge noise. At low concentrations the sensitivity is highest, which gives the best resolution for a device limited by Johnson noise. There is a further limitation, however, because

high dopant concentrations result in lower resistance and therefore higher power consumption for a fixed bias voltage. The sensitivity varies proportionally to the bias voltage (equation (14)), so for a fixed power consumption, a heavily doped cantilever will have reduced sensitivity from the lower bias voltage. This results in a second sensitivity loss associated with higher doping.

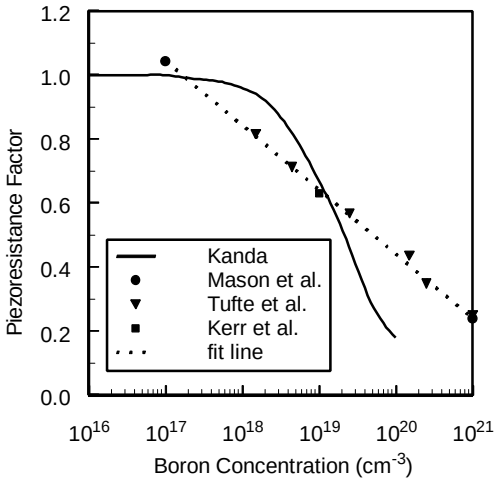

Figure 7. The longitudinal piezoresistive coefficient as a function of boron concentration. The line from Kanda is a theoretical model, the points are experimental data.

For the 1000 Å thick cantilevers in vacuum, we have found that power consumption in excess of 2-3 mW results in destruction of the beams. Thicker cantilevers should be able to dissipate more power, but conservatively assuming a maximum power of 2.5 mW, the optimum doping level can be computed. Figure 8 shows the Hooge and Johnson limited force resolution as a function of dopant concentration for the standard cantilever in a bandwidth from 10 Hz to 1 kHz with a power consumption limited to 2.5 mW. The best force resolution in this case occurs for a doping of 10^{20} cm^{-3}, substantially higher than the 10^{17}-10^{18} cm^{-3} typically used.

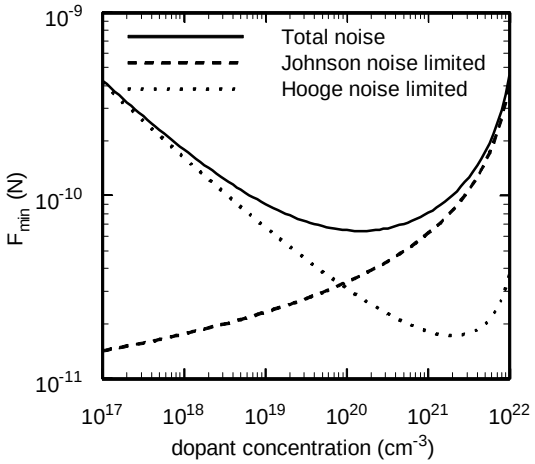

Figure 8. Minimum detectable force vs. doping concentration for standard cantilever[17] assuming a maximum power dissipation of 2.5 mW.

Again, the bandwidth of interest is important. A low-frequency cantilever which is dominated by *1/f* noise will favor heavy doping, while a cantilever used for measurements in a Johnson noise-limited frequency regime will favor low doping. The plot in Figure 9 shows the optimum doping level as a function of the piezoresistor volume and intended bandwidth for $a=10^{-6}$ and P=2.5 mW. To find the optimum doping compute the f_{max}-$f_{min}/log(f_{max}/f_{min})$ for the intended bandwidth and read the doping level from the curve corresponding to the cantilever volume ($l_{leg}t_d w$). This chart should also be valid for piezoresistors of other geometries. The dependence on volume arises because a large cantilever will naturally have more carriers, and can therefore use a lower doping level to increase sensitivity.

High doping levels also have the added advantage of lower sensitivity to temperature fluctuations. Tufte and Stelzer show convincing graphical evidence that as the doping concentration rises, particularly above 10^{20} cm^{-3}, the piezoresistive coefficient becomes almost independent of temperature variations between -80°C and 100°C.

A final consideration for the doping and depth combination is the total resistance, and whether other noise sources may eventually dominate. A good differential amplifier has noise approximately equivalent to the Johnson noise of a 1 kΩ resistor, so1 kΩ is a reasonable value for the minimum acceptable resistance.

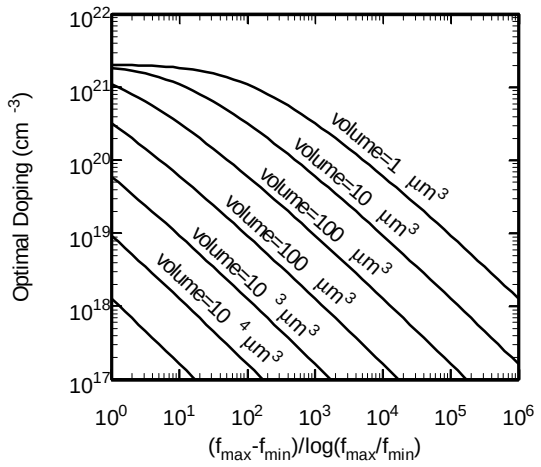

Figure 9. Optimal doping depending on cantilever size and operation bandwidth. A value of 10^{-6} is assumed for α and the power dissipated is 2.5 mW. Compute the value of $(f_{max}-f_{min})/\log(f_{max}/f_{min})$ and read the optimal doping off the y-axis for the given cantilever volume. For other geometry piezoresistors, compute the volume of the conducting region and multiply by 6 to get the equivalent cantilever volume. A 10-fold increase in power consumption is equivalent to a 10-fold decrease in cantilever volume.

Surface Treatment and Anneal

The last important processing decision is the annealing of the dopant, and the potential addition of passivating surface layers. Almost all of the piezoresistive cantilevers discussed in the literature have a passivating oxide layer on the surface of the device, presumably to limit the *1/f* noise due to charge trapping or surface charges (viz. the McWhorter model of *1/f* noise[22]). We found that for the 1000 Å thick piezoresistive cantilevers, a wet etch removal of a 200 Å surface oxide had a negligible effect on the *1/f* noise. While surface noise sources may still be present, and perhaps even dominant in large cantilevers with low Hooge noise, our data supports the claim that there is a bulk *1/f* noise source that eventually limits the cantilevers.

In their study of the *1/f* noise in implanted resistors, Vandamme *et al.* found that annealing could reduce the a parameter of equation (9) by up to three orders of magnitude[23]. The anneal length is therefore another parameter to be optimized. Vandamme *et al.* postulate that the anneal improves the quality of the crystal lattice, thus reducing fluctuations in carrier mobility. Those anneals were for a constant time at varying temperatures, with the conclusion that higher temperature anneals result in a lower a. It is not unreasonable to assume that it is the total anneal, measured in terms of the diffusion length, $\sqrt{Dt}$, which determines the lattice quality. The diffusion coefficient is defined as $D=D_{io}exp(-E_{ia}/k_BT)$, where for boron D_{io}=0.037 cm^2/sec and E_{ia}=3.46 eV[24].

Figure 10 shows a plot of α as a function of anneal from data available in the literature.

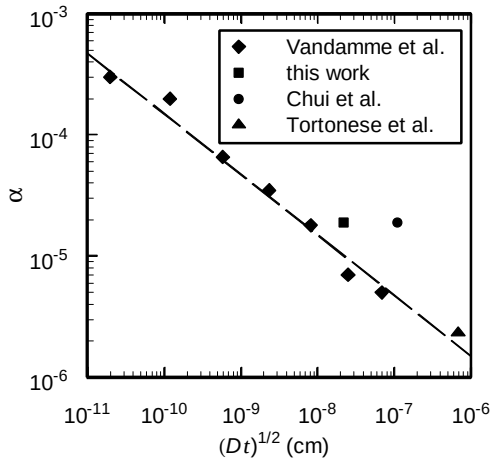

Figure 10. Hooge noise parameter a as a function of anneal diffusion length $\sqrt{D\tau}$. The data from Vandamme *et al.*. was taken on implanted samples annealed for 4 hours at temperatures ranging from 450°C to 900°C [23]; the cantilever from Tortonese *et al.*. was annealed 10 minutes each at 900°C and 1000°C[7]; the cantilever from Chui *et al.*. was annealed 10 seconds at 1000° C and 40 minutes at 800°C[14]; the cantilever from this work was epitaxially grown silicon annealed 3 hours at 700°C[11]. The oxide grown to passivate the epitaxial cantilevers was later removed with pad etch. The other cantilevers remain passivated.

This data is not conclusive, but it does suggest that measured *1/f* levels can be related to the anneal. Since a thermal oxide growth is also an anneal, the importance of surface oxides may actually lie in the improvement of crystal lattice for Hooge noise rather than surface passivation. The data point from Tortonese *et al.* in Figure 4 which was an order of magnitude below the fit line of the rest of the data can now be accounted for by Figure 10, where the a parameter for that work is an order of magnitude better than that of Chui *et al.* and Harley *et al.*

The fit line of Figure 10 is given by $a = 1.5\times10^{-9}\sqrt{\text{cm}}/(Dt)^{1/4}$. An α value of 10^{-6} is the lowest we are aware of, and the indicated trend line is not likely to continue indefinitely. Anneals with $\sqrt{Dt}$ above 10^{-6} cm are therefore perhaps unnecessary. The point from Harley *et al.* is for epitaxially grown silicon, and isn't expected to have the same lattice damage as an implanted sample. These caveats aside, if the indicated line is correct, the result has some interesting implications for optimization.

Much like the argument for the depth of the doped layer, the trade-off here is again between lower *1/f* noise and worsening of b. Longer anneals cause the dopant to diffuse through the beam, resulting in a

distribution which does not experience the maximum possible stress.

Following an implant, the dopant concentration is well approximated by a Gaussian distribution. This distribution spreads as a Gaussian during an anneal, according to

$$p(z,t) = \frac{Q_T}{\sqrt{pDt}} e^{\frac{-z^2}{4Dt}} \qquad (17)$$

where the total implant dopant density is Q_T [cm^{-2}], $\sqrt{Dt}$ is the diffusion length and z is the depth into the surface. It is assumed that the initial implant was done through a surface layer such that $z=0$ occurs at the top of the silicon.

This formula for the concentration can be substituted into equation (6) for b. It is assumed that the implant energy has been selected such that the doping concentration at $z=t/3$ is down a factor of 10 from the surface, or equivalently has a straggle of $\sim t/6.4$. This gives $b \sim 0.7$, which we have previously determined to be nearly optimal. The equation for b can then be plotted as a function of $\sqrt{Dt}$. These results are shown in Figure 11 for an initial peak concentration of $1.5 \cdot 10^{20}$ cm^{-3} for cantilevers of various thicknesses.

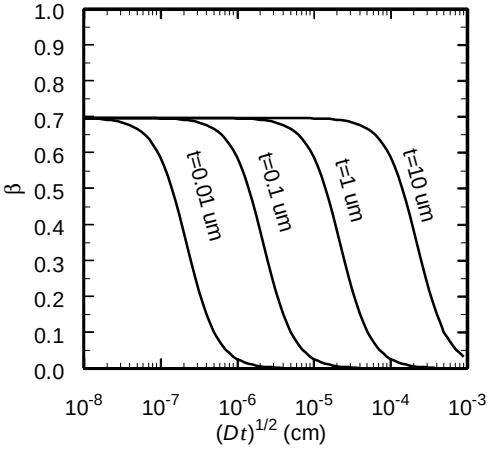

Figure 11. Plot of sensitivity factor β vs. anneal for cantilevers of various thickness. Above the corner frequency for each line, the net resolution worsens, providing an optimum anneal level for a given cantilever thickness.

The most important feature of this figure is that up to some reasonably well defined point the anneal causes negligible dopant diffusion, but beyond this point the sensitivity is substantially reduced. Since the Hooge noise is decreasing with additional annealing, the force resolution improves as long as b is constant. Beyond the corner where b begins to decrease, the *1/f* noise gains are outweighed by sensitivity losses. The optimal anneal strategy is therefore to anneal to the corner of the appropriate curve in Figure 11. For a 1 μm cantilever, the optimal anneal is $\sqrt{Dt} \sim 10^{-5}$ cm. In general, for anneals which are within the range plotted in Figure 10, the optimal anneal as a function of thickness is calculated to be $Dt=0.025t^2$, if t is in meters, and Dt in meters squared. Note, however, that an anneal of $\sqrt{Dt} \sim 2 \cdot 10^{-6}$ cm should achieve a Hooge noise parameter α close to the lowest experimentally observed values. An anneal of $\sqrt{Dt} \sim 2 \cdot 10^{-6}$ cm is therefore likely the maximum required anneal, and should be used for all cantilevers greater than 0.1 μm thick.

Note that this analysis does not include transient enhanced diffusion[25] which can be important for thin implanted cantilevers and would reduce the optimal anneal. A rapid thermal anneal helps reduce transient enhanced diffusion, but does not eliminate it. In contrast to implanted silicon, epitaxially grown silicon has the dopant atoms incorporated into the crystal lattice and is an effective alternative for shallow piezoresistors.

OPERATION

Now that an optimized device has been designed, one final question remains: what is the correct choice of bias voltage for operation? The sensitivity improves linearly with the bias voltage, according to equation (17), so at first glance a high bias voltage appears desirable. For *1/f* noise limited sensing, the noise power varies as V_{bias}^2, so the noise voltage varies as V_{bias} and there should be no preference for a particular bias voltage. The Johnson noise is independent of bias voltage, however, so in this case the higher bias is preferable. With one case preferring high bias, and the other ambivalent, the cantilever should be biased as high as its power dissipation abilities can tolerate. This is typically on the order of a few milliwatts, and is a bias voltage of 5-10 V for most cantilevers. In addition to the potential physical destruction of the cantilever[26], a high operating temperature can also hurt the resolution performance[7].

PREDICTED RESOLUTION

Incorporating all the optimization decisions made so far, we can now estimate the minimum achievable force resolution for piezoresistive cantilevers. Assume the leg lengths extend half the total length, that the width is 10 μm, and that a doped region of 10^{19} cm^{-3} extends one third of the cantilever thickness, giving a b of 2/3. The optimal anneal is then selected as a function of thickness as described previously. For a given thickness and a required spring constant, the length can be determined from equation (4).

The graph in Figure 12 illustrates the displacement resolution vs. thickness for cantilevers of given spring constants. The dashed lines of constant k correspond to the left axis, and indicate the Hooge

limited resolution. The solid lines correspond to the Johnson limited resolution, and are to be read off the right axis. The Hooge limited resolution is given per root-decade of bandwidth since the integrated noise per decade is constant. The Johnson noise is flat vs. frequency, and is therefore given as m/√Hz. Note that once a cantilever is fully limited by *1/f* noise, reduced thickness worsens the resolution, although it may still be advantageous due to bandwidth gains.

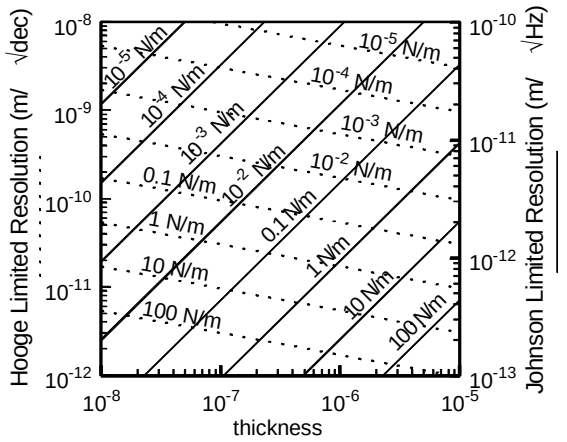

Figure 12. Displacement Resolution, as limited by *1/f* noise and by Johnson noise for 10 μm wide cantilevers. The contours are for constant stiffness, with the spring constant written above the contour. The dotted lines give the *1/f* limited resolution, and the solid lines give the Johnson limited resolution.

EXAMPLE OF CANTILEVER DESIGN

As an example, consider the design of a 0.01 N/m 100 kHz cantilever intended to operate in a bandwidth from 10 Hz up to half its resonance, 50 kHz. From Figure 5, a maximum thickness of 0.2 μm is required. A width of 10 μm is convenient, and from equation (4) the length is set to 70 μm. The legs should extend half the total length and the doping 1/3rd the cantilever thickness. For the bandwidth calculations f_{min}=10 Hz and f_{max}=50 kHz, so the bandwidth figure for Figure 9 is 49990/3.7=13500. The cantilever volume is 134 μm^3, so from Figure 9 the optimal doping will be $4 \cdot 10^{18}$ cm^{-3}. From Figure 11 the anneal should be $\sim 2 \cdot 10^{-6}$ cm.

To calculate the expected displacement resolution this cantilever in a bandwidth from 10 Hz to 50 kHz, compute sqrt(((3·10^{-10} m/√decade)^2 × (3.7 decades)) + ((4·10^{-12} m/√Hz)^2 × (49990 Hz))) to get 1 nm displacement resolution in this bandwidth. Since we have chosen a spring constant of 0.01 N/m, the force resolution is 10 pN.

CONCLUSIONS

Data was shown which validates the Hooge model for *1/f* noise in piezoresistive cantilevers. From equations for the Hooge noise, Johnson noise, and sensitivity, an expression was derived to predict force resolution of a piezoresistive cantilever based on its geometry and processing. Using this expression, an optimization analysis was performed, with the following conclusions:

Design

- The maximum cantilever thickness and the cantilever length will be set by spring constant and bandwidth requirements. For a fixed spring constant the force resolution varies as $w^{1/6}$ and the resonance varies as $w^{-2/3}$, so narrower is preferable, although the effect on resolution is small.
- For piezoresistors limited by Johnson noise, improved resolution can be achieved by reducing the cantilever thickness until, due to processing limitations, b~0.7 can no longer be achieved. For cantilevers limited by *1/f* noise, thicker beams have improved resolution but lower bandwidth.
- The cantilever legs should extend between 30% to 70% of the total length, with shorter legs for Johnson limited devices, and longer ones for *1/f* noise limited cantilevers.

Processing

- The reduction of the piezoresistive coefficient with increased doping is not as severe as is often assumed, and can be expressed according to equation (16).
- The optimal thickness of the doped layer is one third of the total thickness with a 20% loss in resolution for dopant depths of 0.2t and 0.6t.
- For maximum resolution cantilevers should be doped as a function of their bandwidth and volume according Figure 9.
- For cantilevers limited by *1/f* noise the optimal anneal is related to the thickness t according to $D\tau=0.025t^2$, where Dt is in meters squared and t is in meters. Most cantilevers should use an anneal of $\sim 2 \cdot 10^{-6}$ cm, the maximum for which there is experimental Hooge noise data.

Operation

- The cantilever should be operated at as high a bias voltage as its power dissipation can tolerate.

ACKNOWLEDGEMENTS

This work was supported by NSF Career Program (ECS-9502046), the Instrumentation for Materials

Research Program (DMR-9504099), and the DOD Graduate Student Fellowship. The fabrication work made use of the National Nanofabrication Users Network facilities funded by the National Science Foundation under award number ECS-9731294.

REFERENCE LIST

[1] F. J. Giessibl and B. M. Trafas, "Piezoresistive cantilevers utilized for scanning tunneling and scanning force microscope in ultrahigh vacuum," in *Rev. Sci. Inst.*, vol. 65, no. 6, pp. 1923-1929, 1994.

[2] S. C. Minne, J. D. Adams, G. Yaralioglu, S. R. Manalis, A. Atalar, and C. F. Quate, "Centimeter scale atomic force microscope imaging and lithography," in *Appl. Phys. Lett.*, vol. 73, no. 12, pp. 1742-1744, 1998.

[3] R. P. Ried, H. J. Mamin, B.D. Terris, L. S. Fan, and D. Rugar, "5 MHz, 2 N/m piezoresistive cantilevers with INCISIVE tips," in *Transducers 97.1997 International Conference on Solid-State Sensors and Actuators*, 1997, pp. 447-450.

[4] T. Thundat, P. I. Oden, and R. J. Warmack, "Chemical, physical, and biological detection using microcantilevers," in *Proceedings of the Third International Symposium on Microstructures and Microfabricated Systems*, Pennington, NJ, 1997, pp. 179-189.

[5] D. R. Baselt, G. U. Lee, K. M. Hansen, L. A. Chrisey, and R. L. Colton, "A high-sensitivity micromachined biosensor," in *Proc.IEEE*, vol. 85, pp. 672-680, 1997.

[6] M. Tortonese, Force Sensors for Scanning Probe Microscopy, *Ph.D. Thesis*, Stanford University, 1993.

[7] O. Hansen and A. Boisen, "Noise in piezoresistive atomic force microscopy," in *Nanotechnology*, vol. 10, pp. 51-60, 1999.

[8] R. P. Spencer, B. M. Fleischer, P. W. Barth, and J. B. Angell, "A theoretical study of transducer noise in piezoresistive and capacitive pressure sensors," in *IEEE Trans. Electron Devices*, vol. 35, no. 8, pp. 1289-1298, 1988.

[9] H. Nyquist, "Thermal Agitation of Electric Charge in Conductors," in *Phys.Rev.*, vol. 32, pp. 110-113, 1928.

[10] F. N. Hooge, "1/f noise is no surface effect," in *Phys. Lett. A*, vol. 29, pp. 139-140, 1969.

[11] J. A. Harley and T. W. Kenny, "Piezoresistive cantilevers under 1000 Å thick," in *Appl. Phys. Lett.*, vol. 75, no. 2, pp. 289-291, 1999.

[12] C. S. Smith, "Piezoresistance effect in germanium and silicon," in *Phys. Rev.*, vol. 94, no. 1, pp. 42-49, 1954.

[13] L. K. J. Vandamme and S. Oosterhoff, "Annealing of ion-implanted resistors reduces the 1/f noise," in *J. Appl. Phys.*, vol. vol.59, pp. Inclusive-74, 1986.

[14] L. K. J. Vandamme and W. M. G. van Bokhoven, "Conductance noise investigations with four arbitrarily shaped and placed electrodes," in *Appl. Phys.*, vol. 14, no. 2, pp. 205-215, 1977.

[15] T. B. Gabrielson, "Mechanical-thermal noise in micromachined acoustic and vibration sensors," in *IEEE Trans. Electron Devices*, vol. 40, no. 5, pp. 903-909, 1993.

[16] B. W. Chui, T. D. Stowe, T. W. Kenny, H. J. Mamin, B. D. Terris, and D. Rugar, "Low-stiffness silicon cantilevers for thermal writing and piezoresistive readback with the atomic force microscope," in *Appl. Phys. Lett.*, vol. 69, no. 18, pp. 2767-2769, 1996.

[17] Standard cantilever: l=100 μm, w=10 μm, t=1 μm,a=0.5, t_d=t/3, p=10^{19} cm^{-3}, f_{min}=10 Hz, f_{max}=1 kHz

[18] W.P. Mason, J. J. Forst, and L. M. Tornillo, "Recent developments in semiconductor strain transducers," in *Instrument Society of America 15th Annual Conference Proceedings*, New York, 1962, pp. 110-120.

[19] Y. Kanda, "A graphical representation of the piezoresistance coefficients in silicon," in *IEEE Trans. Electron Devices* , vol. 29, no. 1, pp. 64-70, 1982.

[20] O. N. Tufte and E. L. Stelzer, "Piezoresistive Properties of Silicon Diffused Layers," in *J. Appl. Phys.*, vol. 34, no. 2, pp. 313-318, 1963.

[21] D. R. Kerr and A. G. Milnes, "Piezoresistance of diffused layers in cubic semiconductors," in *J. Appl. Phys.*, vol. 34, no. 4, pp. 727-731, 1963.

[22] A. L. McWhorter, *Semiconductor Surface Physics*, University of Pennsylvania Press, Philadelphia, 1957.

[23] L. K. J. Vandamme and S. Oosterhoff, "Annealing of ion-implanted resistors reduces the 1/f noise," in *J. Appl. Phys.*, vol. 59, no. 9, pp. 3169-3174, 1986.

[24] W. R. Runyan and K. E. Bean, *Semiconductor Integrated Circuit Processing Technology*, Addison-Wesley, Reading, MA, 1990.

[25] M. Miyake and S. Aoyama, "Transient enhanced diffusion of ion-implanted boron in Si during rapid thermal annealing," in *J. Appl. Phys.*, vol. 63, no. 5, pp. 1754-1757, 1988.

[26] B. W. Chui, M. Asheghi, Y. S. Ju, K. E. Goodson, H. J. Mamin, and T. W. Kenny, "Intrinsic-carrier thermal runaway in silicon microcantilevers," in *Microscale Thermophys. Eng.*, vol. 3, no. 3, 1999.